

## ADVANCED METHODS FOR THE EVALUATION OF THE HEAT FLUX DISTRIBUTION ONTO THE FIRST WALL OF A TOKAMAK

Fabio Subba and Roberto Zanino

\* Dipartimento di Energetica, Politecnico, Corso Duca degli Abruzzi 24, 10129 Torino, Italy

### ABSTRACT

We present a new computational code for the evaluation of heat fluxes on the first wall of a tokamak reactor. The method applies the Control-Volumes Finite-Element (CVFE) approach to the solution of the plasma fluid equations on the tokamak edge. The CVFE approach is particularly suited for application to triangular meshes, and allows extending the computational grid up to the physical wall of the reactor. As a consequence, it enables studying the Plasma-Wall Interactions (PWI) in full geometrical detail, as opposed to the presently most popular codes, which oversimplify the external wall shape on most of its extension. The new code was developed to study the heat flux deposition onto the IGNITOR First-Wall/Limiter, but has a number of other potential applications, including the limiter start-up phase of the International Thermonuclear Experimental Reactor (ITER), the power deposition onto the external wall driven by Edge Localized Modes (ELMs). Here we discuss the method, illustrate its geometrical potentialities on a simple test case, and present the first application to the analysis of the IGNITOR tokamak first-wall/limiter.

### INTRODUCTION

The IGNITOR [1] First Wall-Limiter (FWL) must withstand the power deposited by the plasma. The relatively small effective area of the solid surfaces available for this task causes the heat flux onto the wall to be large. IGNITOR will produce about 20 MW of fusion power, to be exhausted on a surface of  $\sim 34 \text{ m}^2$ , with a peak heat flux above  $1 \text{ MW} / \text{m}^2$ . The combination of thermal and mechanical stresses onto the Plasma-Facing Components (PFC) can severely limit the expected lifetime of these components, with negative influences on the machine maintenance costs. For this reason, it is important to evaluate the power distribution on the FWL with great accuracy under different operating conditions, in order to help an effective wall design.

A number of sophisticated numerical codes exist to study the PWI in a tokamak [2-4], but most of them are optimised for a divertor configuration, and their application to IGNITOR is difficult. In fact, the use of magnetic-fitted coordinates in modelling an edge plasma tokamak allows important simplifications for a divertor machine, provided a very crude treatment of the outer wall, far from the target plates, is tolerated. This is compromise is often accepted in divertor tokamak modelling, based on the assumption that the critical region for PWI is the divertor itself.

However, the IGNITOR design does not include a divertor, and the outer wall should be studied in detail in all its extension. Furthermore, the confined plasma is in direct contact with the solid walls along a line where the wall itself is tangent to the magnetic field, which would add considerable problems if magnetic fitted co-ordinates had to be adopted.

In addition, even if it is true that in other machines a considerable part of the PWI is localized in the divertor region, the correct control of the outer wall interactions with the plasma can still play an important role. For example, at JET there is experimental evidence that a large fraction of the

energy expelled from the plasma during the so-called Edge Localized Modes (ELMs) is deposited onto the outer wall [5]. In addition, the typical ITER shot will have a limiter during the start-up and shutdown phases [6].

In this paper we present the code ASPOEL, under development at Politecnico di Torino with the aim of providing sufficient geometrical flexibility to model properly the IGNITOR edge plasma, including its FWL, and to allow for an accurate evaluation of the heat flux distribution. In the next section, we recall the equations constituting the most common edge plasma fluid models. Then we discuss in some detail the geometrical problems, which prevent from the successful application of the most popular codes available, and the additional flexibility introduced by the CVFE method implemented in ASPOEL. After that we discuss the application of the ASPOEL code to a reference case in a somewhat simplified geometry. Then we illustrate the first application to the IGNITOR experiment and, finally, we draw our conclusions.

### MODEL EQUATIONS

The physical model usually adopted in modelling the macroscopic behaviour of edge tokamak plasmas is a hydrodynamic model describing a mixture of charged fluids in a strong magnetic field. Due to the magnetization, the transport coefficients are strongly anisotropic, transport being impeded normal to the field [7]. The electric current flowing in the plasma is not strong enough to perturb appreciably the field itself, which can be considered externally imposed, within a very good accuracy. Furthermore, fluid analysis is interested in macroscopic spatial scales (larger than the plasma Debye length), and the fluid motion does not reach relativistic velocities. Finally transport normal to the magnetic field lines is not treated on a first principle basis, but is included mostly via a diffusive ansatz. The above conditions

allow formulating a standard set of equations for edge tokamak plasma [8].

We consider the case of only one, singly charged ion species present in the plasma, and assume the electron and ion temperatures to be the same. In this case, the equations to be solved are:

$$\frac{\partial n_i}{\partial t} + \nabla \cdot (n_i \bar{u}_i) = 0 \quad (1)$$

$$n_e = n_i \quad (2)$$

$$\frac{\partial \Gamma_{\parallel,i}}{\partial t} + \bar{e}_{\parallel} \cdot \nabla \cdot (\bar{\Gamma}_i \bar{u}_i + p_i \hat{I} + \hat{\pi}_i) = 0 \quad (3)$$

$$n_i u_{r,i} = -D_r \nabla_r n_i \quad (4)$$

$$\bar{u}_e = \bar{u}_i \quad (5)$$

$$\frac{\partial}{\partial t} \left( \frac{3}{2} n_e k_B T_e \right) + \nabla \cdot \left( \frac{5}{2} n_e k_B T_e \bar{u}_e + \bar{q}_e \right) = 0 \quad (6)$$

$$T_i = T_e \quad (7)$$

Equation (1) is the continuity equation for ions. An analogous expression for electrons is substituted by equation (2), called quasi-neutrality. Equation (3) is the parallel component of the ion momentum equation. Perpendicularly to the magnetic field, equation (4) describes the ion particle flux by means of a diffusive ansatz, while equation (5) states that there is no net current in the plasma. Equation (6) describes the electron energy transport, and finally equation (7) states that the ion and electron temperatures are equal. We solve equations (1)-(7) in a poloidal cross-section of the machine, taking advantage from the assumption of toroidal symmetry.

Parallel to the field, transport is mostly collisional, and is described satisfactorily by the classical theory [7]. No satisfactory theory for the transport perpendicular to the field exists, and here we assume the corresponding coefficients to be constant for the sake of simplicity. The ion pressure  $p_i$  is related to the density and temperature by the ideal gas law. For the ease of the reader, in the following we will sometimes express the temperature in eV units, as is customarily done in the plasma literature.

## COMPUTATIONAL IMPLICATIONS

To make a simple estimate, we can assume the electron thermal diffusivity parallel to the magnetic field in plasma to be given by [9]:

$$\chi_{\parallel} \sim \frac{2000}{en_e} \left( \frac{k_B T}{e} \right)^{5/2} \text{ m}^2/\text{s} \quad (8)$$

while, in the perpendicular direction, a value

$$\chi_r \sim 0.3 \text{ m}^2/\text{s} \quad (9)$$

is common. The edge plasma temperature is usually at least a few  $10^4$  K, but increases rapidly moving towards the plasma centre. In the cold outer plasma regions the density can be a few  $10^{19} \text{ m}^{-3}$ . With such numbers, the ratio of the parallel to the perpendicular heat diffusivities is of the order of  $10^3$ . In reality, due to its strong temperature dependence, it will

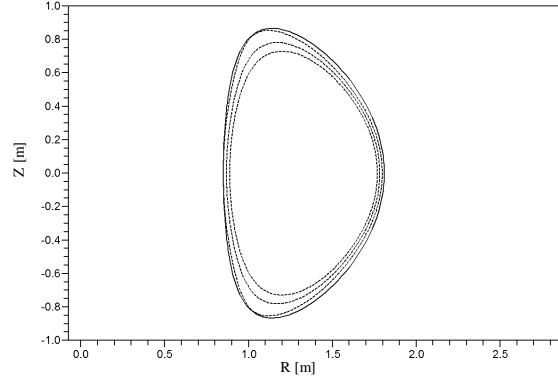


Figure 1. The IGNITOR equilibrium with some of the most external magnetic surfaces in the plasma. The last line is the outer wall

increase dramatically in the inner edge regions. The magnetic field lines in a tokamak lie on a set of nested magnetic surfaces, as shown in figure 1, where they are represented by lines in a poloidal cross section crossing the machine symmetry axis. Any reasonable edge plasma computational code must have a mesh aligned with the magnetic field, in order to deal with such a strong anisotropy with an acceptable number of nodes.

All the most popular edge plasma codes in use today deal with the plasma anisotropy by solving the plasma equations with the Finite Volume (FV) technique in a curvilinear orthogonal co-ordinate system, where the magnetic field lines (or, equivalently, their projection on the machine cross-section) provide one set of co-ordinate lines. We refer conventionally to such co-ordinate system as  $(\theta, r)$ ,  $\theta$  being the poloidal (i.e. curvilinear along the magnetic lines projection) co-ordinate, and  $r$  the radial one. While this solution has the advantage of accounting for the anisotropy in a very efficient way, serious problems arise at the walls, which do not, in general, coincide with a co-ordinate line. Divertor target plates can be represented as  $\theta = \text{const.}$  lines, provided the requirement of an orthogonal system is relaxed (however, some very popular plasma codes assume explicitly an orthogonal system [2], so that relaxing this hypothesis can cause some concern [10]). On the other hand, the representation as a  $\theta = \text{const.}$  line of the outer wall, usually built with the minimum possible incidence angle to the magnetic field in order to distribute the thermal load as uniformly as possible, is not practical. In most cases, the wall is then approximated as a field line, i.e. as an  $r = \text{const.}$  line. The drawback of this solution is that the geometrical details of the outer wall are lost. This has been considered an acceptable compromise for a long time, but today there is increasing experimental evidence of strong interactions between the plasma and the wall far from the target plates [5], and the wall will play an even more important role in the ITER reactor [6]. Furthermore, tokamaks like IGNITOR and TEXTOR [11] do not rely on the divertor concept, so that this approach is not suitable in that case.

Some attempts at providing increased geometrical flexibility, while retaining the framework of the magnetic co-ordinates exist [11], but have been applied so far only to limited wall portions. At the other extreme, triangular unstructured meshes can, in principle, provide the required flexibility. Triangular Finite Elements (FE) are a possible alternative, which was explored in [12] and [13], up to

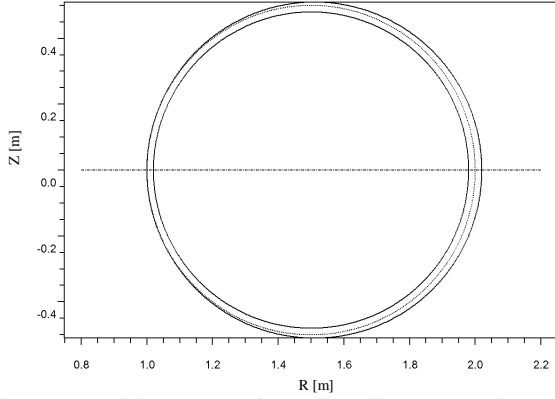


Figure 2 Model cross section adopted to create the test case discussed in the text. Solid lines: the outer wall and the inner plasma boundary. Dashed line: the LCFS. Dotted line, the up-down symmetry axis. The inner plasma boundary has been moved inwards to allow distinguishing it from the LCFS.

producing a comparison of code results with experimental data, however without including in the domain the complete outer wall.

We are moving further on using triangular meshes, by developing the ASPOEL code, based on the Control-Volume Finite Elements (CVFE) approach [14]. The method works on triangular meshes, dividing the computational domain in a set of control volumes (CV) obtained by joining the centres of the elements, as exemplified in figure 3. As in the standard FV method, the CVFE approach is based on the local application of the fluid conservation laws for each CV. To this aim, a prescription is needed on how to reconstruct the fluxes crossing the CV boundaries. We obtain this by interpolating the primary variables (velocity, pressure and temperature) on each element using properly chosen shape functions, as in the FE approach. This produces an expression for the primary variables on the whole domain, with values at the mesh nodes as degrees of freedom. Such expression can be used to compute the fluxes at the CV boundaries. The method derives its flexibility from the FE approach, retaining the conservativeness proper of the FV technique.

In order to build the mesh, we select first a set of magnetic surfaces. Then we place a number of computational nodes on each surface and, finally we connect the nodes into a triangular mesh, with the additional requirement that no

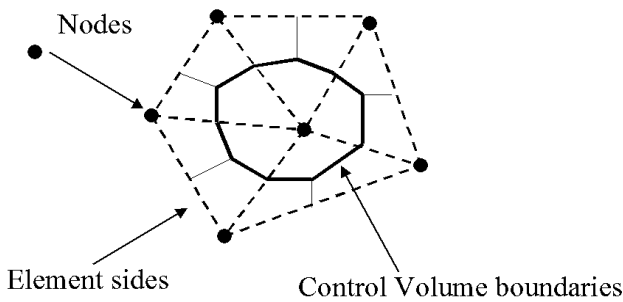


Figure 3. A mesh of triangular elements (dashed lines) is used to generate a set of control volumes (solid lines) surrounding each node. Control volumes are built by joining the centres of each triangle with the mid-points of the surrounding sides.

element edge can cross any of the selected magnetic surfaces. This procedure generates a triangular mesh, each element of which has an edge lying on a magnetic surface.

To select the interpolating functions, we adopt for each element a local orthogonal ( $l_\theta, r$ ) co-ordinate system. Then we write the interpolating function on each element as:

$$f = a + b \exp(P_{e,g} l_g / L_g) + c \exp(P_{e,r} r / L_r) \quad (10)$$

where the (directional) mesh Peclet numbers  $P_{e\theta}$  and  $P_{e,r}$  are defined as:

$$P_{e,g} = \frac{V_g L_g}{\delta_{//}} \quad (11)$$

$$P_{e,r} = \frac{V_r L_r}{\delta_r} \quad (12),$$

with  $V_{\theta(r)}$  the flow speed in the poloidal (radial) direction,  $\delta_{//(\perp)}$  the parallel (radial) diffusivity (of momentum, when solving equation (3) or of energy in equation (6)), and  $L_{\theta(r)}$  the element extension. The constants a, b, and c are chosen to match the value of the interpolating function at the element vertices with the value of the primary variable to be represented. This choice, together with the particular construction of the mesh elements, reflects the natural separation between poloidal and radial directions in the plasma, and accounts for the possibly varying relative strength of convection and diffusion processes in different domain regions [14].

The system of algebraic equations resulting from the discretization procedure is linearized with a segregated approach. During the iterations, the momentum and continuity equations are coupled with the SIMPLE algorithm [15], in the formulation proposed in [2] for the particular form of the plasma fluid equations.

## APPLICATION TO A TEST CASE

We describe here the application of the ASPOEL code to a reference case in order to illustrate, in a somewhat simplified case, the geometrical problems discussed above and the solution obtained with the CVFE approach.

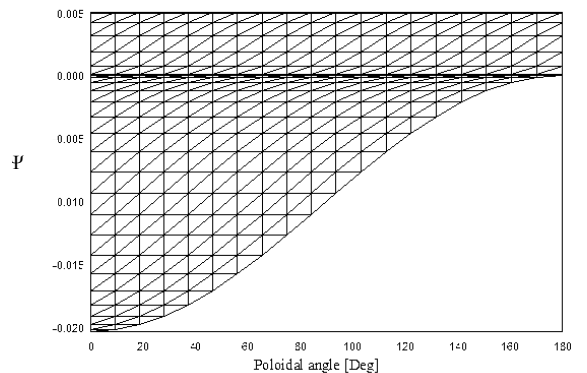


Figure 4. Computational domain and mesh for the model problem described, represented in the  $(\theta, \psi)$  space

	Continuity	Parallel momentum	Electron energy
Inner plasma	$n_i = 2 \times 10^{20} \text{ m}^{-3}$	$V_{  } = 0 \text{ m/s}$	$T_e = 55 \text{ eV}$
Outer wall	$V_r = 0.01$ $V_{th,i}$	$V_{  } = c_s$	$q_{e,  } = 5nc_sT_e$
Inboard mid-plane	-	$V_{  } = 0 \text{ m/s}$	adiabatic
Outboard mid-plane	-	$V_{  } = 0 \text{ m/s}$	adiabatic

Table 1 Boundary conditions adopted for the model problem.

We consider a model tokamak, whose magnetic surfaces are perfectly circular coaxial tori, with major axis  $R_0 = 1.5 \text{ m}$ . The outer wall is a further circular torus, with the same up-down symmetry plane as the magnetic configuration (we label it as the  $Z = 0$  plane) but with major and minor radii  $R_w = 1.51 \text{ m}$  and  $r_w = 0.51 \text{ m}$ , respectively. Inside the plasma, we extend our domain up to the value

$$r_{in} = 0.495 \text{ m} \quad (13)$$

With the mentioned data, the poloidal cross section of the Last Closed Flux Surface (LCFS) is a circle internally tangent to the outer wall at the  $Z = 0$  location, as illustrated in figure 2. The magnetic field runs on the magnetic surfaces with a constant pitch angle:

$$\frac{B_g}{B} = 0.1 \quad (14)$$

We conventionally label the magnetic surfaces with the coordinate

$$\Psi = 0.25 - r^2 \quad (15)$$

Equation (15) assigns the value  $\Psi = 0$  to the LCFS, and characterizes the Scrape-off Layer (SOL) with the condition  $\Psi < 0$ , as is often done in tokamak studies. The particular geometry chosen allows building an orthogonal mesh with reduced efforts: we simply adopt a cylindrical mesh in the cross-section plane with origin in the magnetic axis. The resulting mesh is best viewed in the  $(\theta, \Psi)$  plane, as shown in figure 4.

We solved equations (1) – (7) in the upper half of the model domain, taking advantage of the problem up-down

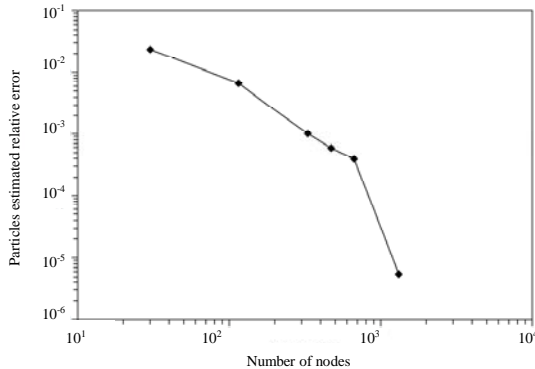


Figure 5 Estimated relative error in the particles entering the SOL as a function of the number of nodes.

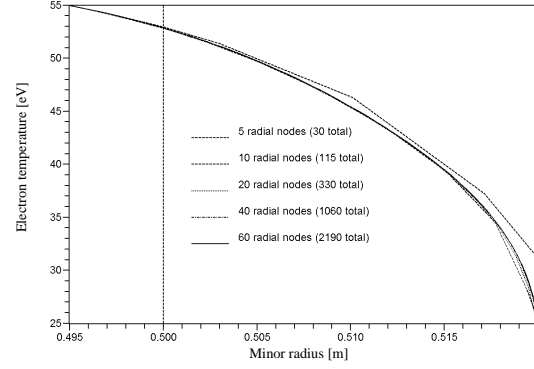


Figure 6. Radial temperature (in eV) profiles at the outboard mid-plane on different meshes. The vertical line marks the LCFS

symmetry. We list in table 1 the boundary conditions chosen. Both the geometrical dimensions and the boundary conditions of the model problem were chosen to reproduce roughly the operative conditions expected for IGNITOR. Conditions at the inner plasma boundary were set to be compatible with the edge parameters estimated in [16]. At the outer wall, the condition on the parallel momentum is almost standard in the literature [9], as opposed to the condition on the radial velocity component, for which the available analysis is very limited. We adopted the prescription proposed in [17], based on a kinetic model. At the inboard/outboard mid-planes, we choose the conditions in order to preserve the problem symmetry.

The radial transport coefficients also were selected to be compatible with the expected IGNITOR values. We used:

$$D_r = 0.3 \text{ m}^2 / \text{s} \quad (16)$$

$$\chi_r = 4.5 \text{ m}^2 / \text{s} \quad (17)$$

$$\eta_r = 0.3 \text{ m}^2 / \text{s} \quad (18)$$

for the particle, energy and momentum radial diffusivities, respectively.

We studied the spatial convergence of the code by monitoring the rate of particles and the power entering SOL from the inner plasma. Figures 5 and 7 show the observed reduction in the relative error estimate as a function of the number of nodes. The error estimate was obtained by comparing the result computed on the different meshes with an estimate of

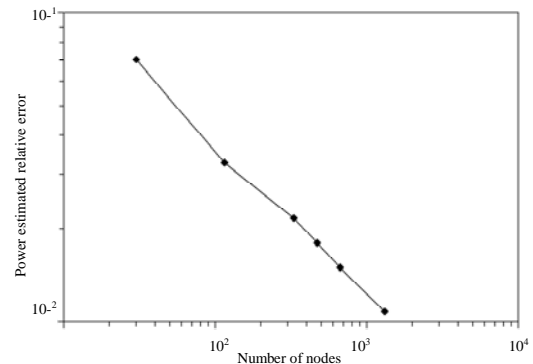


Figure 7. Estimated relative error in the power entering the SOL as a function of the number of nodes.

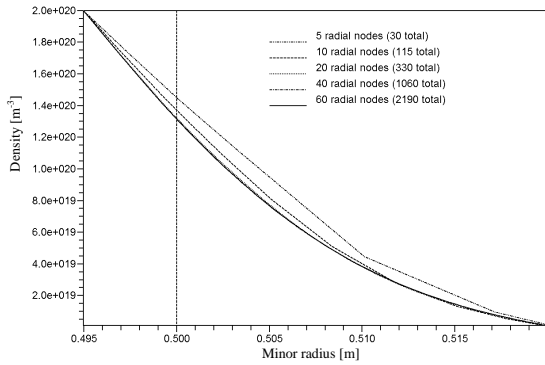


Figure 8. Radial density profiles at the outboard mid-plane on different meshes. The vertical line marks the LCFS

the mesh-independent value obtained by Richardson extrapolation [18]. Both particles and power are stabilizing towards a final value, even if with different velocities. In figures 6 and 8 we also show the temperature and density radial profiles at the outboard mid-plane on different meshes. In addition to the total number of nodes, in each figure the meshes are classified by the number of radial nodes in the SOL (counted at the outboard mid-plane), as an alternative measure of the mesh resolution.

## APPLICATION TO IGNITOR

We briefly discuss now the first application to IGNITOR of the ASPOEL code. Figure 9 shows the IGNITOR wall in the  $(\theta, \psi)$  space, with  $\psi$  the poloidal magnetic flux. Besides the tangency point between the wall and the LCFS (marked by  $\psi = 0$ ) there is, at the inboard mid-plane, a second location where the LCFS runs very close to the wall, at about  $110^\circ$ . This results in an almost complete division of the SOL in two secondary SOLs, each of which was meshed independently.

We studied a case with the same boundary conditions and transport coefficients discussed in the previous section. In figures 10 and 11 we show the radial density and temperature profiles computed at the outboard IGNITOR mid-plane. Both curves are compared with an exponential profile with characteristic length 8 mm, which is often assumed to be comparable with the SOL width in IGNITOR. Both profiles show a substantial decrease across the SOL, but it is clear that the existence of a truly exponential profile is questionable.

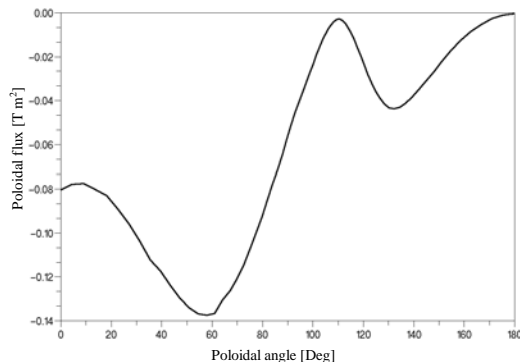


Figure 9. The IGNITOR wall represented in the  $(\theta, \psi)$  space.

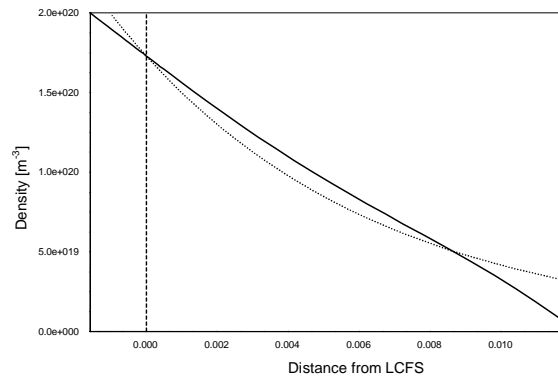


Figure 10 Radial density profiles for IGNITOR at the outboard mid-plane. An exponential with characteristic length 8 mm is also shown for comparison (dashed). The vertical line marks the LCFS position.

This is not completely surprising, because exponential profiles are usually derived based on simplified geometrical hypothesis, which are not satisfied in a real machine. Furthermore, even in the simpler case discussed in the previous section, the existence of exponential profiles was not guaranteed, especially for the temperature. Finally, in figure 12 we show the heat flux distribution onto the IGNITOR outer wall, distinguishing the parallel and the radial contributions. The latter is often neglected in tokamak modelling, on the basis of the strong anisotropy of the plasma transport coefficients. However, a relevant contribution, similar to the one we found, in the regions where parallel transport is deleted by geometrical effects (i.e. at the tangency between the wall and the magnetic surfaces) is experimentally observed [19].

## CONCLUSIONS

We have discussed the implementation of the CVFE method in the ASPOEL code, for modelling the IGNITOR edge plasma with acceptable geometrical accuracy. We adopt triangular FE meshes, as some previous attempts, but retain the conservativeness of the classical FV method, on which most edge plasma codes are based. While developed purposely for IGNITOR, the code is in principle suitable to

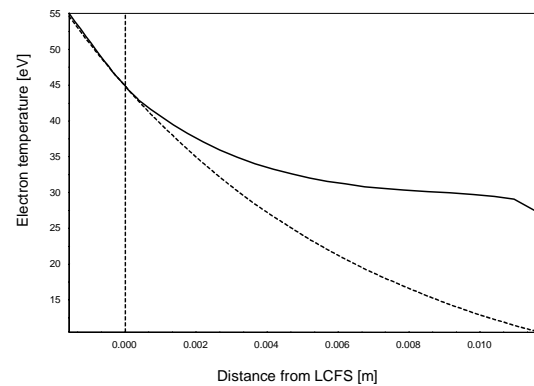


Figure 11 Radial temperature profiles for IGNITOR at the outboard mid-plane. An exponential with characteristic length 8 mm is also shown for comparison (dashed). The vertical line marks the LCFS position.

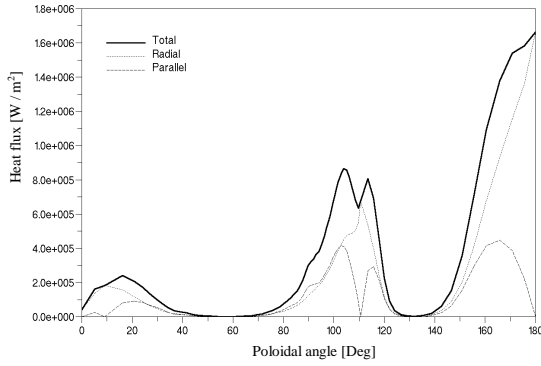


Figure 12. Computed heat flux distribution along the IGNITOR first wall

study also divertor plasma, including a complete representation of the First Wall.

The physics included in the model is a simplification of the most developed models implemented in more sophisticated edge codes (e.g. drifts and diamagnetic transport are not considered), but it contains enough physics to allow a critical assessment of the method. We discussed in some length the application to a benchmark case, to study the convergence of the method. On this case, the method proved to be sufficiently robust. A preliminary application of the code to an IGNITOR case has also been reported, demonstrating the possibility to extend the domain of a fluid edge plasma model up to the first wall/limiter.

## NOMENCLATURE

Symbol	Quantity	SI Unit
$n_i$	ion density	$m^{-3}$
$u_i$	ion velocity	$m/s$
$n_e$	electron density	$m^{-3}$
$\Gamma$	ion momentum	$kg\ m/s$
$e_{//}$	magnetic field unit vector	-
$p$	ion pressure	Pa
$\pi$	ion stress tensor	Pa
$D_{//}(\tau)$	parallel (radial) particle diffusivity	$m^2/s$
$u_e$	electron velocity	$m/s$
$k_B$	Boltzmann constant	J/K
$q_e$	electron heat flux	$W/m^2$
$T_e$	electron temperature	K
$T_i$	ion temperature	K
$\chi_{//}(\tau)$	parallel (radial) heat diffusivity	$m^2/s$
$\eta_r$	radial momentum diffusivity	$m^2/s$
$\delta_{//}(\tau)$	parallel (radial) diffusivity	$m^2/s$

## REFERENCES

[1] G. Cenacchi, and A. Airoidi, *Equilibrium Configurations for the IGNITOR Experiment*, Rapporto ENEA FP01/1, (2001).

[2] B.J. Braams, *A Multi-Fluid Code for Simulation of the Edga Plasma in Tokamaks*, NET Report EUR-FU/XII-80/87/68, (1987).

[3] R. Simonini, G. Corrigan, G. Radford, J. Spence, and A. Taroni, *Models and Numerics in the Multi-Fluid 2-D Edge Plasma Code EDGE2D/U*, Contributions to Plasma Physics, **34**, (2/3), 368-373, (1994).

[4] T.D. Rognlien, *A Fully Implicit, Time Dependent 2-D Fluid Code for Modeling Tokamak Edge Plasmas*, Journal of Nuclear Materials, **196-198**, 347-451, (1992).

[5] T. Eich, A. Herrmann, G. Pautasso, P. Andrew, N. Asakura, J.A. Boedo, Y. Corre, M.E. Fenstermacher, J.C. Fuchs, W. Fundamenski, G. Federici, E. Gauthier, B. Goncalves, O. Gruber, A. Kirk, A.W. Leonard, A. Loarte, G.F. Matthews, J. Neuhauser, R.A. Pitts, V. Riccardo, C. Silva, *Power deposition onto plasma facing components in poloidal divertor tokamaks during type-I ELMs and disruptions*, Journal of Nuclear Materials, **(337-339)**, 669-676, (2005).

[6] ITER Physics Expert Group on Divertor, ITER Physics Expert Group on Divertor Modelling and Database, Iter Physics Basis Editors, ITER EDA, *ITER Physics basis. Chapter 4: power and particle control*, Nuclear Fusion **39**, (12), 2391-2469, (1999).

[7] S.I. Braginskii, *Transport Processes in a Plasma*, Reviews of Plasma Physics, ed. M.A. Leontovich, Consultants Bureau, New York, (1965).

[8] R. Schneider, X. Bonnin, K. Borrass, D.P. Coster, H. Kastelewicz, D. Reiter, V.A. Rozhansky, and B.J. Braams, *Plasma Edge Physics with B2-Eirene*, Contributions to Plasma Physics, **46**, (1-2), 3-191, (2006).

[9] P.C. Stangeby, *The Plasma Boundary of Magnetic Fusion Devices*, Institute of Physics Publishing, (1999).

[10] F. Subba, and R. Zanino, *Modeling plasma-wall interactions in First Wall-Limiter geometry*, Computer Physics Communications, **164**, 377-382, (2004).

[11] M. Baelmans, D. Reiter, B. Kueppers, P. Boerner, *Plasma edge fluid models for recycling at near tangential surfaces*, Journal of Nuclear Materials, **290-293**, 537-541, (2001).

[12] R. Zanino, *Advanced Finite Element Modeling of the Tokamak Plasma Edge*, Journal of Computational Physics, **138**, 881-906, (1997).

[13] R. Marchand, F. Meo, M. Simard, B. Stansfield, E. Haddad, G. Abel, J.L. Lachambre, D. Pinsonneault, N. Richard, TdeV team, *Finite element modelling Da radiation and impurity transport in tdev*, Journal of Nuclear Materials, **266-269**, 1129 - 1133, (1999).

[14] B.R. Baliga, *Control-Volume Finite Element Methods for Fluid Flow and Heat Transfer*, Advances in Numerical Heat Transfer, **1**, 97-135, (1996).

[15] S.V. Patankar, *A Calculation Procedure for Heat, Mass and Momentum Transfer in Three-Dimensional Parabolic Flows*, International Journal of Heat and Mass Transfer, **15**, 1787-1806, (1972).

[16] R. Zanino, *Effects of High-Z Limiter/First Wall on the IGNITOR Plasma*, DENER Report PT DE 501/IN, (1999).

[17] K. Teilhaber, and C. Birdsall, *Kelvin-Helmoltz Vortex Formation and Particle Transport in a Cross-field Plasma Sheath. II. Steady state*, Physics of Fluids B, **1**, (11), 2260-2272, (1989).

[18] P.J. Roache, *Quantification of Uncertainty in Computational Fluid Dynamics*, Annual Review of Fluid Mechanics, **29**, 123-160, (1997).

[19] C.S. Pitcher, P.C. Stangeby, M.G. Bell, J.D. Elder, S.J. Kilpatrick, D.M. Manos, S.S. Medley, D.K. Owens, A.T. Ramsey and M. Ulrickson, *Plasma fluxes to surfaces for an oblique magnetic field*, Journal of Nuclear Materials, **196-198**, 241-247, (1992).